Published in final edited form as:
Mol Cell. 2014 June 19; 54(6): 920–931. doi:10.1016/j.molcel.2014.04.013.

H2B ubiquitylation promotes RNA Pol II processivity through regulating PAF1 and pTEFb pathways

Lipeng Wu[#1], **Li Li**[#3], **Bo Zhou**[1], **Zhaohui Qin**[3], and **Yali Dou**[1,2,*]

[1]Department of Pathology, University of Michigan, Ann Arbor, MI 48109, USA

[2]Department of Biological Chemistry, University of Michigan, Ann Arbor, MI 48109, USA

[3]Department of Biostatistics and Bioinformatics, Rollins School of Public Health, Emory University, Atlanta, GA 30322, USA

[#] These authors contributed equally to this work.

SUMMARY

Histone H2B ubiquitination plays an important role in transcription regulation. It has been shown that H2B ubiquitination is regulated by multiple upstream events associated with elongating RNA polymerase. Here we demonstrate that H2B K34 ubiquitylation by the MOF-MSL complex is part of the protein networks involved in early steps of transcription elongation. Knocking down MSL2 in the MOF-MSL complex affects not only global H2BK34ub, but also multiple co-transcriptionally regulated histone modifications. More importantly, we show that the MSL, PAF1 and RNF20/40 complexes are recruited and stabilized at active gene promoters by direct binary interactions. The stabilized complexes serve to regulate chromatin association of pTEFb through a positive feedback loop and facilitate Pol II transition during early transcription elongation. Results from our biochemical studies are underscored by genome-wide analyses that show high RNA Pol II processivity and transcription activity at MSL target genes.

Introduction

Covalent modifications of histones play an integral role in transcription regulation, which underlie many important cellular processes. Recent studies suggest close coordination between histone modifications and transcription machineries at each regulatory steps of gene expression including initiation, elongation, termination and eventually transcription re-initiation (Campos and Reinberg, 2009; Lee and Young, 2013; Suganuma and Workman, 2013). Transition of RNA pol II from initiating to elongating complex, which is marked by increased phosphorylation of Serine 2 within the conserved `YSPTSPS' motif of its carboxyl-terminal domain (CTD) (Fuchs et al., 2009; Phatnani and Greenleaf, 2006), is accompanied by dynamic changes of histone modifications along the transcribed regions.

[*]**Correspondence:**yalid@umich.edu, Tel: (734) 6151315, Fax: (734) 7636476.

For example, promoter enriched histone acetylation gradually gives way to co-transcriptionally regulated H3 lysine (K) K36 methylation and H2B K120 ubiquitylation (K120ub) as transcription machineries move into gene coding regions (Campos and Reinberg, 2009; Li et al., 2007). The co-transcriptionally regulated histone modifications facilitate chromatin dynamics in the wake of Pol II passage and re-establish nucleosome phasing to suppress cryptic transcription, both of which enhance productive transcription. The converging point of transitions of Pol II and histone modifications is under extensive studies, which reveal interplays among multiple chromatin modifying enzymes and transcription elongation factors (Bataille et al., 2012; Buratowski, 2009).

A prominent feature of RNA Pol II transition at early transcription elongation stage is promoter-proximal pausing (Core and Lis, 2008; Glover-Cutter et al., 2008). Pol II pausing is the rate-limiting step for a large subset of genes (e.g. ~30% in hESCs) in metazoan (Adelman and Lis, 2012; Lis, 2007; Rahl et al., 2010) and it serves as a checkpoint that coordinates transcription elongation, chromatin modifications as well as mRNA processing (Adelman and Lis, 2012). The positive transcription elongation factor b (pTEFb), a heterodimer consisting of a cyclin and a cyclin dependent kinase CDK9, is proposed to be the central player in releasing RNA Pol II from pausing and moving Pol II into productive elongation phase (Bres et al., 2008; Pirngruber et al., 2009). Genetic studies in yeast shows that Bur1, the CDK9 ortholog in yeast, mediates phosphorylation of Spt5 (Liu et al., 2009; Zhou et al., 2009), that serves to recruit the Paf1C (Jaehning, 2010; Laribee et al., 2005; Tomson and Arndt, 2013). Paf1C, in turn, regulates Rad6/Bre1 mediated H2BK123 ubiquitylation (Laribee et al., 2005; Wood et al., 2005) and phosphorylation of Ser2 (Ser2p) of Pol II CTD through the Rif1 (Restores TBP function 1) (Piro et al., 2012; Tomson et al., 2011) and Ctr9 or Cdc73 (Cell Division Cycle 73) subunits respectively (Chu et al., 2007; Nordick et al., 2008). Therefore, Bur1 and Paf1C are critical players for the transition of Pol II into the elongation phase. In higher eukaryotes, many proteins in this regulatory pathway are conserved (Jaehning, 2010; Tomson and Arndt, 2013) and direct interactions between PAF1C and RNF20/40 (mammalian Bre1) as well as PAF1C dependent H2BK120ub are reported (Kim et al., 2009; Kim et al., 2010; Kim and Roeder, 2009). However, the regulatory pathways upstream of PAF1C, especially the functional interactions between PAF1C and pTEFb in mammals remain unclear. Furthermore, it is also unclear if PAF1C and pTEFb play roles in regulating a more complex H2Bub network beyond H2BK120ub (Tweedie-Cullen et al., 2009; Wu et al., 2011).

Our previous study shows that the MSL1/2 heterodimer in the mammalian MSL complex (also called MOF-MSL) has an E3 ubiquitin ligase activity for H2BK34 (Wu et al., 2011). However, little is known for the function and regulation of this novel H2B ubiquitylation mark in cells. Specifically, although the MSL complex is implicated in transcription elongation from studies of the homologous Drosophila dMSL complex (also called dosage compensation complex DCC) (Conrad and Akhtar, 2011; Gelbart and Kuroda, 2009; Lucchesi et al., 2005), which show enrichment of dMSL at coding regions of male X-linked genes (Alekseyenko et al., 2006; Gilfillan et al., 2006; Kind et al., 2008) and interactions with H3K36me (Soruco et al., 2013; Sural et al., 2008), direct link of the MSL or dMSL complexes with transcription cofactors that are specific for either initiation or elongation steps have not been reported. The lack of biochemical characterization of the MSL complex

in transcription regulation makes it difficult to unequivocally determine the critical role of the MSL complex in this process despite extensive genome-wide profiling studies of the dMSL complex (Conrad et al., 2012; Ferrari et al., 2013; Larschan et al., 2011; Straub and Becker, 2013; Vaquerizas et al., 2013).

Here we have carried out rigorous *in vitro* biochemical studies to demonstrate the direct and extensive physical interactions between the MSL complex and the pTEFb-PAF1C transcription regulatory pathway in mammalian cells. Furthermore, we discover an interdependent regulatory network and positive feedback loop among pTEFb, PAF1C and H2Bub in early transcription elongation. Genome-wide studies further support the functions of the MSL complex in facilitating RNA Pol II travel at coding regions and enhancing overall transcription activity of its target genes. Taken together, our studies establish a role of the mammalian MSL complex during early transcription elongation. Given the conservation of the MSL complex as well as PAF1C and pTEFb, the results here will have broad implications for the function of MSL and H2Bub in transcription regulation in higher eukaryotes.

RESULTS

Development of the anti-H2BK34ub antibody

Our previous studies have identified a novel histone ubiquitin ligase activity for the MSL1/2 heterodimer in the MSL complex. The MSL complex targets histone H2BK34, which further stimulates H3K4 methylation by MLL1/hSET1 and H3K79 methylation by DOT1L *in vitro* (Wu et al., 2011). In order to test whether H2BK34ub is indeed present in mammalian cells, we developed a polyclonal antibody for this histone mark using a similar strategy as previously described for the generation of anti-H2BK120ub antibody (Minsky et al., 2008). As shown in Figure 1A, the anti-H2BK34ub antibody specifically recognizes a branched peptide corresponding to the conjugation site (K34) of ubiquitin on histone H2B, but not the unmodified H2B peptide in the dot blot analyses. To further confirm its specificity, we performed immunoblot using increasing concentrations of chemically synthesized H2BK120ub protein (McGinty et al., 2008). Although H2BK120ub can be readily detected by anti-H2BK120 antibody, no detectable cross-reactivity was found for anti-H2BK34ub antibody under the same condition (Figure 1B).

The MSL complex ubiquitylates H2BK34ub in cells

Using the anti-H2BK34ub antibody, we set to confirm MSL1/2 mediated H2BK34ub both *in vitro* and in cells. We first set up the *in vitro* ubiquitylation assay using recombinant E1, E2 (UBC5c or Rad6) and HA-ubiquitin (HA-Ub) as previously described (Wu et al., 2011). The RNF20/40 complex, the E3 ubiquitin ligase for H2B K120 (Kim et al., 2009), was included as a control. As shown in Figure 1C, both MSL and RNF20/40 showed robust E3 ubiquitin ligase activity on nucleosomal H2B as detected by the anti-HA antibody. No histone ubiquitylation was detected in their absence (Figure 1C, lane 1). When we used the anti-H2BK120ub or anti-H2BK34ub antibodies to probe ubiquitylation products, H2BK120ub was detected only when RNF20/40 was added as the E3 ubiquitin ligase (Figure 1C, lane 3). Similarly, H2BK34ub was detected when MSL1/2, but not RNF20/40, was added as the E3

ubiquitin ligase in in vitro assays (Figure 1C, lane 2). These results further confirmed specificity of anti-H2BK34ub antibody as well as substrate selectivity for RNF20/40 and MSL1/2 *in vitro* (Wu et al., 2011).

We next tested whether H2BK34ub is present in mammalian cells and whether this modification is mainly regulated by MSL. To this end, we isolated core histones from HeLa cells treated with or without MSL2 knockdown. As shown in Figure 1D, depletion of MSL2 by siRNA in HeLa cells completely abolished global H2BK34ub, suggesting that MSL2 is the major E3 ubiquitin ligase for this histone modification in cells. Similar results were also obtained from embryonic stem cells (ESCs) and 293 cells (Supplemental Figure 1 and 2), suggesting prevalence of this histone mark in mammals. Consistent with our previous results, knocking down MOF in the MSL complex did not affect global H2BK34ub (Figure 1D).

Mutual dependence of MSL1/2 and RNF20/40

Since we previously showed that MSL1/2 affected global H2BK120ub in cells (Wu et al., 2011), we next examined whether RNF20/40 functions downstream of MSL1/2. To this end, we treated 293 cells with RNF20 and RNF40 shRNAs and examined global H2BK34ub. To our surprise, depletion of RNF20/40 not only abolished H2BK120ub, but also led to dramatic reduction of global H2BK34ub in cells (Figure 2A). Down regulation of H2BK34ub by RNF20/40 knockdown was not due to changes at the MSL2 protein level (Supplemental Figure 2B) or non-specific recognition by the antibody (Figure 1). This result, together with MSL1/2 regulation of H2BK120ub (Wu et al., 2011), suggests that H2BK120ub by RNF20/40 and H2BK34ub by MSL1/2 are mutually dependent. To understand the mechanism for this mutual dependency, we examined chromatin association of RNF20 or MSL2 after knocking down the reciprocal E3 ligase. To this end, lysates from cells treated with control, RNF20 or MSL2 siRNAs were fractionated into chromatin and soluble fractions. The distribution of proteins in each fraction was examined by immunoblot. We found that MSL1/2 knockdown led to redistribution of RNF20 to the soluble fraction (Figure 2B, lane 1 vs. 3). Conversely, depletion of RNF20/40 resulted in decrease of MSL2 chromatin binding as well (Figure 2B, lane 1 vs. 2). These results suggest that chromatin recruitments of RNF20/40 and MSL1/2 are inter-dependent, which indirectly affect their respective H2Bub activity in cells.

To our surprise, RNF20/40 or MSL1/2 knockdown also led to decreased chromatin binding of PAF1 and CDK9 in mammalian cells (Figurer 2B), contrary to the well-characterized PAF1C-dependent RNF20/40 pathway in yeast and *in vitro* (Kim et al., 2009; Kim et al., 2010). We decided to further study whether PAF1 regulates RNF20/40 and MSL1/2 in a reciprocal manner in mammals. As shown in Figure 2C, knocking down PAF1 in HeLa cells led to dramatic decrease of both global H2BK34ub and H2BK120ub (Figure 2C), which were due to decreased chromatin binding of RNF20 and MSL2 (Figure 2D). Consistent with PAF1 regulation of the MSL complex, PAF1 knockdown also led to global reduction of H4K16ac and H2Bub dependent H3 K4 and K79 methylation in these cells. In sum, the RNF20/40, MSL and PAF1C complexes are functionally inter-dependent and subject to extensive feedback regulations in mammalian cells.

Direct interactions among MSL1/2, RNF20/40 and PAF1 complexes

To explore the molecular mechanism of the functional inter-dependence, we expressed and purified individual components of the RNF20/40, MSL and PAF1 complexes and set up coimmunoprecipitation (IP) experiments to detect direct physical interactions among them *in vitro*. We first incubated Flag-tagged recombinant MOF, MSL1, MSL2 or MSL3 protein individually with the purified RNF20/40 complex and subject them to M2 affinity purification. As shown in Figure 3A, MSL1, but not other components of the MSL complex, directly interacted with the RNF20/40 complex. The reciprocal co-IP experiment using Flag-tagged RNF20 or RNF40 and MSL1 proteins showed that MSL1 predominantly interacted with RNF20 in the RNF20/40 complex (Figure 3B). We had also detected interactions between endogenous MSL1 and RNF20 or RNF40 by IP using anti-MSL1 antibody (Supplemental Figure 3A). No interaction with RNF20/40 complex was detected for endogenous MSL2, MSL3 or MOF under our IP conditions (Supplemental Figure 3A). Detailed mapping of MSL1 identified its N-terminus (1-221aa) as the essential domain for interacting with RNF20 (Figure 3C). Hence, the MSL and RNF20/40 complexes physically associate with each other through direct MSL1-RNF20 interactions.

Next, we examined direct interactions between the MSL and PAF1 complexes *in vitro*. To this end, we expressed Flag-tagged PAF1, CTR9, LEO1, CDC73, RTF1 or Ski8 proteins and mixed them individually with the purified MSL1/2 complex. Direct interactions between PAF1 and MSL1, and to a lesser extent MSL2, were observed (Figure 4A). Reciprocal IP using Flag-tagged MSL1, MSL2, MSL3 and MOF also confirmed PAF1-MSL1 as well as PAF1-MSL2 interactions (Figure 4B). Furthermore, when we examined interactions among endogenous proteins, we found that anti-MSL1 antibody most efficiently precipitated endogenous PAF1 (Supplemental Figure 3B), consistent with the co-IP results. In conclusion, PAF1 directly interacts with the MSL complex with preference for MSL1. Mapping of direct interaction domains showed that a fragment of MSL1 283-472aa and the MSL2 C-terminus were involved (Figure 4C and 4D). Importantly, the domains in MSL1 that were mapped for PAF1 and RNF20 interactions were different, suggesting that these two interactions are not mutually exclusive. These results suggest that PAF1 regulates H2Bub by physically tethering both RNF20/40 and the MSL complex to chromatin.

Since both RNF20/40 and the MSL complex interact with PAF1C, we decided to test whether the pair-wise interactions could be further stabilized by the presence of the third factor(s). To this end, we first performed co-IP experiment for Flag-PAF1 in the presence of RNF20/40 or the MSL complex or both complexes together. As shown in Figure 5A, interactions between PAF1 and RNF20 or PAF1 and MSL1 were greatly enhanced in presence of the second E3 complex (lane 3 vs. 2 and lane 6 vs. 5). Similar conclusions can be drawn when we performed co-IP experiments for Flag-MSL1 and either RNF20/40, PAF1 or both complexes together (Figure 5B, lane 2 vs. 3, 4). These results suggest that MSL1/2 and RNF20/40 cooperate with each other in their interactions with the PAF1 complex, supporting interdependent chromatin associations among these complexes (Figure 2B and 2D).

Feedback regulations of pTEFb and H2Bub

Genetic studies in yeast shows that Bur1, the CDK9 ortholog in yeast, mediates recruitment of Paf1C (Laribee et al., 2005),(Jaehning, 2010; Tomson and Arndt, 2013), which in turn regulates H2BK123ub (Laribee et al., 2005),(Wood et al., 2005). This is concurrent with pTEFb mediated transition of Pol II into productive elongation. To explore whether pTEFb regulates MSL1/2 mediated H2BK34ub in mammalian cells, we first knocked down CDK9 and examined global histone modifications by immunoblot. CDK9 knockdown led to global reductions of H2BK34ub and H2BK120ub as well as the downstream H3 K4 and K79 methylation (Figure 5C). Consistent with a direct regulation of the MSL complex by pTEFb, CDK9 knockdown also reduced global H4K16ac by MOF (Figure 5C). The regulation was at the step of chromatin association since knocking down CDK9 led to increased dissociation of MSL2, RNF20 and PAF1 from chromatin (Figure 5D). Of note, although CDK9 has recently been shown to phosphorylate Pol II Ser5p (Bartkowiak et al., 2010; Czudnochowski et al., 2012; Ghamari et al., 2013), knocking down CDK9 did not change chromatin-associated Pol II Ser5p. Instead, it led to reduction in Pol II Ser2p (Figure 5D), consistent with what was previously reported in the literature (Jaehning, 2010; Pirngruber et al., 2009). The reduction of chromatin associated Pol II Ser2 could be due to indirect effects of CDK9 knockdown (see discussion). Interestingly, we found a reciprocal regulation of CDK9 chromatin binding by the PAF1C and H2Bub. Knocking down any of these proteins led to dissociation of CDK9 from chromatin as well as reduction of Pol II Ser2p (Figure 5E and Figure 2). These results revealed a novel feedback regulation between H2Bub and pTEFb in mammals.

To further understand the mechanism underlies functional interactions between CDK9 and H2Bub, we examined whether there were direct physical interactions among the complexes. We were not able to detect any direct pair-wise interactions between CDK9 and RNF20/40 or the MSL complex or PAF1C (data not shown). However, we found that CDK9 has higher affinity for H2B ubiquitylated by MSL1/2 as compared to unmodified H2B *in vitro* (Supplemental Figure 4A). Consistently, MSL1/2 ubiquitylation activity is essential to stabilize chromatin binding of CDK9 (Figure 5F). When we knocked down MSL2 in HeLa cells followed by overexpression of either wild type or the catalytically inactive $MSL2^{H64Y}$, only wild type exogenous MSL2 was able to restore CDK9 chromatin binding (Figure 5F, lane 3). In contrast, inactive $MSL2^{H64Y}$ mutant was not able to rescue CDK9 chromatin binding (Figure 5F, lane 4). As control, overexpression of $MSL2^{H64Y}$ restored RNF20 chromatin binding (Figure 5F), suggesting no requirement of MSL2 enzymatic activity. Levels of Pol II CTD Ser2p correlated with pTEFb chromatin binding in all cases (Figure 5F). These results suggest that CDK9 binding to chromatin at least in part depends on its direct interactions with H2BK34ub.

Mutual dependent recruitment of MSL1/2, PAF and pTEFb complexes at *HOXA9* and *MEIS1* loci

To confirm that interplays among components of the pTEFb-H2Bub pathway occurred at gene specific levels, we examined MSL2, RNF20, PAF1, or CDK9 binding at *HOXA9* and *MEIS1* loci by chromatin immunoprecipitation (ChIP). Both genes are well-established direct targets for these protein complexes (Wu et al., 2011; Zhu et al., 2005). To this end, we

performed CHIP assays for each of the key components of the pathway after knocking down the rest of pathway proteins (Figure 6A–E). Consistent with global changes, recruitment of the MSL, RNF20/40, PAF1C and pTEFb complexes to *HOXA9* and *MEIS1* loci were interdependent at 5' end of *HOXA9* and *MEIS1* genes. Knocking down key components of each protein complex led to significant decrease in bindings of other complexes at both gene loci (Figure 6A–D). Reduction of Ser2-phosphorylated (Figure 6E), but not Ser5-phosphylated Pol II (Figure 6F), at both gene loci was observed as well. Modest reduction of H3K36me2 was also found at gene bodies of *HOXA9* and *MEIS1* (Supplemental Figure 4B). ChIPs at Oct4 gene locus, which is transcriptionally silent in HeLa cells, were used as the negative control. Taken together, these results suggest that the MSL complex is an integral part of a network essential for regulating elongating Pol II in mammals.

Genome-wide analyses of MSL binding sites in mammalian cells

To assess global functions of the MSL complex in transcription regulation, we performed genome-wide ChIP-seq experiment for Msl2 in murine embryonic stem cells (mESCs). The results were directly compared to previously reported Mof (GSE37268) and RNA Pol II binding sites (GSE20485) (Li et al., 2012; Rahl et al., 2010). The ChIP-seq results showed that mammalian Msl2 were enriched on all autosomes in the mammalian genome (Supplemental Figure 5A). About 30% Msl2 peaks physically overlap with previously identified Mof binding peaks in mESCs (Supplemental Figure 5B). Gene pathways for the joint Mof and Msl targets were summarized in Supplemental Figure 5C. We further examined Msl2 distribution relative to the gene structure. To this end, we divided the genome into eight categories: 5' distal (2–100kb upstream of transcription start site (TSS), 5' proximal (0–2kb upstream of TSS), 5'UTR (TSS to ATG), coding, 3'UTR (TGA to transcription end site (TES)), 3' proximal (0–2kb downstream of TES) and 3' distal (2–100kb downstream of TES) regions respectively. The rest were referred to as inter-genic regions. As shown in Figure 7A, consistent with a role in transcription elongation, majority of Msl2 binding sites (~50.6%) were mapped to the transcribed region in the genome including ~42.5% peaks in coding regions, ~5.9% in 5'UTR and ~2.2% in 3' UTR respectively. The rest were at either distal or inter-genic regions whose functional significance remained to be explored. Interestingly, the distribution of the MSL complex (defined by joint Msl2 and Mof binding peaks) is similarly to that of Pol II CTD Ser2p on the scaled gene body, with higher binding at TSS and TES (Figure 7B). We further analyzed the MSL binding peaks within a 12kb region surrounding the annotated TSS. To this end, the joint Mof/Msl2 peaks were counted and grouped into 24 bins with 500bp intervals starting from −2kb to +10kb regions. Similar to RNA Pol II CTD Ser2p, Mof/Msl2 peaks centered on TSS but also distributed broadly throughout the 10kb region downstream of TSS, (Figure 7C). Heat map of ChIP-seq peaks around TSS (+/− 3kb) further confirmed significant genome wide correlation among the Msl complex and Pol II Ser2p (Figure 7D). Taken together, the CHIP-seq study supports a role of the MSL complex in transcription elongation, consistent with our biochemical studies *in vitro*.

MSL binding correlates with higher Pol II traveling rate and transcription activity

To gain mechanistic insights on MSL in gene regulation, we next examined whether the Msl complex contributes to RNA Pol II transition from initiation to elongation. To this end, we

employed the concept of pol II traveling ratio (TR) that was previously discussed (Zeitlinger et al., 2007). Pol II traveling ratio (TR) is defined as the ratio of Pol II binding at the promoter-proximal region vs. the gene body. It is also referred to as the pausing index in the literature (Rahl et al., 2010; Reppas et al., 2006). Basically, lower TR value reflects less Pol II pausing and higher efficiency of Pol II transition from initiation to elongation. We decided to examine Pol II TR value at targets of the MSL complex (defined by joint Msl2 and Mof peaks) or non-Msl Mof targets and non-Mof targets respectively. The Pol II TR of each group was calculated and the percentage of genes vs. TR value was plotted in Figure 7E. Interestingly, target genes of the Msl complex (red) had significantly lower Pol II TR value than that of Mof alone (black) or non-Mof (blue) targets with *p* value at 4.023e-13 and 4.391e-13 respectively (Wilcoxon Signed-rank test). About 50% actively transcribed targets of the Msl complex have TR of less than 10, in contrast to ~ 30% for non-Msl target genes (Figure 7E). The Msl targets also had significantly higher overall expression level as compared to non-Msl targets (Supplemental Figure 6, p=1.834e-14, Wilcoxon signed-rank test) (see discussion). Taken together, the unbiased genome wide CHIP-seq experiment shows that the Msl complex probably functions to facilitate Pol II transition from initiation to elongation, which leads to more productive transcription.

Knocking down MSL2 leads to decreased Pol II binding at gene bodies

Since Pol II TR value reflects combined effects of transcription initiation, attainment of Pol II processivity and transcription termination, we decided to directly test at which step the Msl complex affects Pol II binding to its target genes. To this end, we selected four genes in murine ESCs that are direct Msl targets (i.e. Mbd3, Uba52) or non-Msl Mof targets (i.e. Med21) or non-Mof targets (i.e. Crebl2) from the CHIP-seq experiments (Supplemental Figure 7A). Knocking down either Msl2 or Mof genes led to down regulation of Mbd3 and Uba52 while only Mof knockdown led to down regulation of Med21. Neither knockdown affected Crebl2 expression (Supplemental Figure 7B and 7C). As shown in Supplemental Figure 7, knockdown of Mof led to reduction of Pol II binding at both TSS and coding regions of Mbd3, Uba52 and Med21. In contrast, Msl2 knockdown led to reduction of Pol II only at gene bodies of Mbd3 and Uba52 (p-values are 0.014 and 0.0083 respectively, Supplemental Figure 7D and 7E). No change of Pol II peaks at TSS was detected (p-values are 0.97 and 0.74 resepctively). As the control, Pol II binding at Crebl2 or Med21 gene was not affected by Mof or Msl2 knockdown. These results support that the MSL complex is an integral component of the regulatory network for transcription elongation.

Discussion

Here we report extensive biochemical characterizations of the MSL complex and its interaction with transcription elongation factors PAF1C, pTEFb and H2B E3 ubiquitin ligase RNF20/40. The binary interactions between MSL and PAF1C or RNF20/40 serve to stabilize their chromatin binding, which, together with H2Bub, regulate pTEFb and Pol II CTD Ser2p through a positive feedback loop. These results not only establish a novel function of the MSL complex in transcription regulation, but also suggest that histone H2B ubiquitination is involved in regulating Pol II processivity through feedback regulation of pTEFb and PAF1C. Our biochemical studies are further underscored by revelation that

direct MSL targets have lower RNA Pol II pausing index and higher transcription activity in the genome-wide analyses.

Role of the MSL complex in transcription elongation

The mammalian MSL complex has two conserved histone modifying activities: H4K16ac by MOF and H2BK34ub by MSL1/2 (Wu et al., 2011). However, despite well-characterized enzymatic activities, little is known for the function of the MSL complex in transcription regulation, especially its interaction with basic transcription machinery. In order to gain mechanistic insights, we have examined direct and functional interactions of the MSL complex with the regulatory pathways important for early transcription events. Several lines of evidence from our studies support a role of the MSL complex in transcription elongation: 1) MSL1 and to a lesser extent, MSL2, directly interact with PAF1C; 2) MSL1 directly interacts with RNF20/40; 3) binary interactions between MSL1/2 and RNF20/40 or PAF1C further stabilizes PAF1C-RNF20/40 interaction and are important for their chromatin recruitment; 4) MSL and its ubiquitylation activity are important for chromatin association of pTEFb; and finally 5) genome-wide analyses show strong correlations of MSL binding with high Pol II processivity in cells. In sum, our study here establishes the direct link between the MSL complex and transcription elongation in higher eukaryotes. Of note, given the function of PAF1 in multiple transcription-related processes including transcription initiation (Tomson and Arndt, 2013), it is possible that the MSL complex is involved in multiple stages of transcription regulation as well, which will be of interest for future studies. Since MSL and transcription elongation factors discussed in this study are highly conserved, it will be interesting to examine whether our conclusion here can be extended to other eukaryotic system, especially the Drosophila dMSL complex.

Feedback regulation of early transcription elongation

Pol II pausing, demonstrated by the presence of promoter proximal peaks, is a prominent feature of early transcription elongation in higher eukaryotes (Adelman and Lis, 2012). Extensive studies show that Pol II pausing is the result of active regulation that involves transcription elongation factors DSIF (Spt4 and Spt5) and NELF (Adelman and Lis, 2012). Spt5 in the DSIF complex is phosphorylated by yeast Bur1 and mammalian CDK9 in the pTEFb complex. Alternatively, Pol II pausing is proposed to be a result of slow Pol II transition into elongation complex at early transcription stage (Ehrensberger et al., 2013). Regardless of the exact mechanism, our studies show that PAF1-MSL-RNF20/40 complexes as well as H2Bub play important roles in facilitating Pol II release from pausing (as marked by Pol II CTD Ser2 phosphorylation), probably through cooperative regulation of chromatin binding of the pTEFb complex. Notably, we believe down regulation of Pol II Ser2p after CDK9 knockdown is probably due to indirect effects since CDK9 has been shown to phosphorylate Ser5 of Pol II CTD and Pol II Ser2p in mammals is mainly carried out by CDK12 (Bartkowiak et al., 2010; Czudnochowski et al., 2012; Ghamari et al., 2013).

Our studies here reveal extensive binary interactions and feedback controls among transcription elongation factors and H2Bub. Each factor in this network (e.g. PAF1C, MSL2) including H2Bub is involved in feedback controls of both up- and down-stream factors and eventually regulates Pol II CTD Ser2p. This is in contrast to S. cerevisiae, where

mechanistic studies have depicted a linear regulatory pathway that starts with Spt5 phosphorylation by Bur1 kinase and ends with H2Bub dependent H3 methylation. Depletion of any factor in this pathway leads to disruption of downstream process and eventual loss of H3 methylation (Jaehning, 2010; Tomson and Arndt, 2013). Our study points to the presence of a complex regulation network in early transcription elongation in mammals. It is consistent with increasing complexity of higher eukaryotes and expanding roles for multiple proteins of this pathway in diverse biological processes including tumorigenesis, embryonic development, cell survival and maintenance of ESCs (Ding et al., 2009; Johnsen, 2012; Kelland, 2000; Trujillo and Osley, 2012). We also notice a recent work in *S. pombe* (Sanso et al., 2012) that shows the presence of feedback regulations among most of the factors we discussed here, suggesting the evolution conservation of the network.

Redundant functions of H2B ubiquitylation

Both H2BK120ub and H2BK34ub are well characterized in their regulation of histone H3 K4 and K79 methylation (Laribee et al., 2007; Osley, 2004; Weake and Workman, 2008; Wu et al., 2011). Interestingly, they rarely co-localize on one histone H2B since di-ubiquitylated H2B was not detected by immunoblot (data not shown). Here we show that both H2BK34ub and K120ub are regulated by the same set of transcription elongation factors and show mutual dependency in their recruitment to target genes as well as their enzymatic activities in cells. This is largely due to direct physical interactions between MSL1 and RNF20 as well as their cooperative binding to PAF1. Furthermore, both H2BK34ub by the MSL complex and H2BK120ub by RNF20/40 contribute to recruitment/retention of pTEFb on chromatin as well as the processivity of RNA Pol II. We would like to point out that we are not able to identify specific functions associated with individual H2Bub event, raising the questions on whether they function redundantly in cells and why cells need two intertwined enzymatic complexes for the same function. One possible explanation for this multiplicity is to increase the robustness of the system. Indeed, precedence for built-in redundancy in eukaryotic system is well established. An alternative explanation is that regulatory networks comprised of cooperative interactions allows for better signal integration and fine-tuning (Ruthenburg et al., 2007). Consistent with this view, the direct PAF1-RNF20/40 interaction in higher eukaryotes is relatively weak (Kim et al., 2010) and can be dramatically enhanced by interacting with MSL as we described here or by WAC protein as previously reported (Zhang and Yu, 2011). The development of parallel or inter-related pathways in regulating early transcription elongation events is probably a necessary response to vastly increased complexity during evolution, which warrant future studies.

Experimental Procedure

Plasmids and Recombinant Proteins

The Plasmids of MSL1 and its various domain fragments, MSL2 and its fragments, MSL3, and CDK9 were also subcloned into pFastBac vectors. Baculovirus were generated according to the manufacturer's instruction (Gibco-Invitrogen).

In vitro Histone Ubiquitination and co-Immunoprecipitation (co-IP) Assays

In vitro histone ubiquitination assays were performed as previously described (Wu et al., 2011). For in vitro co-IP experiments, the purified proteins including components from the PAF1 complex, the RNF20/40 complex and the MSL complex were mixed as indicated in binding buffer (20mM Tris-Cl [pH 7.9], 300mM KCl, 20% glycerol, 0.1%NP-40, 0.5mg/ml BSA). The mixture was incubated with M2 beads for 3 hours. After extensive wash, the bound proteins was eluted with 20 mM Flag peptide and detected by immunoblot.

Chromatin Fractionation and Immunoprecipitation Assays

For chromatin isolation, the Hela cell pellets were suspended sequentially in buffer A (10mM Hepes [ph7.9], 10mM KCl, 1.5mM $MgCl_2$, 0.34M Sucrose, 10% Glycerol, 0.1% TritonX-100) for 5 minutes and then buffer B (10mM Hepes [ph7.9], 10mM EDTA) for 30 minutes. The supernatant was collected as cytoplasmic and nucleoplasmic fraction, respectively. The remaining pellet was dissolved in loading buffer as chromatin fraction. For immunoprecipitation, endogenous MSL1, MSL2, MSL3, MOF were pulled down with specific antibody in binding buffer (20mM Tris-Cl [pH 7.9], 300mM KCl, 20% glycerol, 0.1%NP-40), and the bound proteins was separated on SDS-PAGE and detected by immunoblot.

siRNA mediated Knockdown experiment

For knockdown experiments, cells were transfected with siRNA duplex (Dharmacon) using Oligofectamine (Invitrogen) according to the manufacturer's instruction. The siRNA for RNF20, RNF40, CDK9 and PAF1 are listed in Table S1. The siRNA against MSL1 and MSL2 were described previously (Wu et al., 2011).

ChIP assay, real time RT-PCR and ChIP-Seq Analyses

ChIP assays performed at *HOXA9* and *MEIS1* loci were described previously (Dou et al., 2005). Primers for quantitative RT-PCR were summarized in Table S2 and S3 respectively. ChIP-seq analysis for MSL2 was performed at University of Michigan Sequencing Core Facility. The CHIP-seq data were deposited in NCBI database with the Bioproject ID PRJNA242648, which include input (SRR1205106) and MSL2 ChIP (SRR1205109). ChIP-seq reads were mapped to mouse reference genome mm9 using Bowtie (Langmead et al., 2009), allowing no more than single mismatch. ChIP-seq peaks were analyzed using HPeak (Qin et al., 2010), a hidden Markov model-based algorithm for identifying CHIP-enriched region. Peaks from different samples within distance of 200bp are defined as overlapped peaks. The ChIP-seq data sets for Pol-II were obtained from National Center for Biotechnology Information Gene Expression Omnibus (NCBI GEO) database under accession number GSE20485. The ChIP-seq datasets for MOF and Microarray dataset were published previously under accession number GSE37268. Traveling ratio was calculated as described previously (Rahl et al., 2010). Other analysis methods including heat map, bar plot, box plot, and enrichment count were also applied as indicated. Wilcoxon Signed-rank test or Spearman's correlation coefficient was used for calculating p values when evaluating significance of difference.

Supplementary Material

Refer to Web version on PubMed Central for supplementary material.

Acknowledgments

We would like to thank Drs Jaehoon Kim and Robert G. Roeder for providing expression vectors for PAF1, CTR9, LEO1, CDC73, RTF1, SKI8, RNF20 and RNF40 as well as antibodies against RNF20 and RNF40. We also thank Dr. Tom Muir for providing the H2BK120ub protein. This work is supported by NIGMS R01 (GM082856), American Cancer Society Research Scholar (ACS), Leukemia and Lymphoma Society Scholar grants to YD.

REFERENCE

Adelman K, Lis JT. Promoter-proximal pausing of RNA polymerase II: emerging roles in metazoans. Nat Rev Genet. 2012; 13:720–731. [PubMed: 22986266]

Alekseyenko AA, Larschan E, Lai WR, Park PJ, Kuroda MI. High-resolution ChIP-chip analysis reveals that the Drosophila MSL complex selectively identifies active genes on the male X chromosome. Genes Dev. 2006; 20:848–857. [PubMed: 16547173]

Bartkowiak B, Liu P, Phatnani HP, Fuda NJ, Cooper JJ, Price DH, Adelman K, Lis JT, Greenleaf AL. CDK12 is a transcription elongation-associated CTD kinase, the metazoan ortholog of yeast Ctk1. Genes Dev. 2010; 24:2303–2316. [PubMed: 20952539]

Bataille AR, Jeronimo C, Jacques PE, Laramee L, Fortin ME, Forest A, Bergeron M, Hanes SD, Robert F. A universal RNA polymerase II CTD cycle is orchestrated by complex interplays between kinase, phosphatase, and isomerase enzymes along genes. Mol Cell. 2012; 45:158–170. [PubMed: 22284676]

Bres V, Yoh SM, Jones KA. The multi-tasking P-TEFb complex. Curr Opin Cell Biol. 2008; 20:334–340. [PubMed: 18513937]

Buratowski S. Progression through the RNA polymerase II CTD cycle. Mol Cell. 2009; 36:541–546. [PubMed: 19941815]

Campos EI, Reinberg D. Histones: annotating chromatin. Annu Rev Genet. 2009; 43:559–599. [PubMed: 19886812]

Chu Y, Simic R, Warner MH, Arndt KM, Prelich G. Regulation of histone modification and cryptic transcription by the Bur1 and Paf1 complexes. Embo J. 2007; 26:4646–4656. [PubMed: 17948059]

Conrad T, Akhtar A. Dosage compensation in Drosophila melanogaster: epigenetic fine-tuning of chromosome-wide transcription. Nat Rev Genet. 2011; 13:123–134. [PubMed: 22251873]

Conrad T, Cavalli FM, Vaquerizas JM, Luscombe NM, Akhtar A. Drosophila dosage compensation involves enhanced Pol II recruitment to male X-linked promoters. Science. 2012; 337:742–746. [PubMed: 22821985]

Core LJ, Lis JT. Transcription regulation through promoter-proximal pausing of RNA polymerase II. Science. 2008; 319:1791–1792. [PubMed: 18369138]

Czudnochowski N, Bosken CA, Geyer M. Serine-7 but not serine-5 phosphorylation primes RNA polymerase II CTD for P-TEFb recognition. Nat Commun. 2012; 3:842. [PubMed: 22588304]

Ding L, Paszkowski-Rogacz M, Nitzsche A, Slabicki MM, Heninger AK, de Vries I, Kittler R, Junqueira M, Shevchenko A, Schulz H, et al. A genome-scale RNAi screen for Oct4 modulators defines a role of the Paf1 complex for embryonic stem cell identity. Cell Stem Cell. 2009; 4:403–415. [PubMed: 19345177]

Dou Y, Milne TA, Tackett AJ, Smith ER, Fukuda A, Wysocka J, Allis CD, Chait BT, Hess JL, Roeder RG. Physical association and coordinate function of the H3 K4 methyltransferase MLL1 and the H4 K16 acetyltransferase MOF. Cell. 2005; 121:873–885. [PubMed: 15960975]

Ehrensberger AH, Kelly GP, Svejstrup JQ. Mechanistic interpretation of promoter-proximal peaks and RNAPII density maps. Cell. 2013; 154:713–715. [PubMed: 23953103]

Ferrari F, Jung YL, Kharchenko PV, Plachetka A, Alekseyenko AA, Kuroda MI, Park PJ. Comment on “Drosophila dosage compensation involves enhanced Pol II recruitment to male X-linked promoters”. Science. 2013; 340:273. [PubMed: 23599463]

Fuchs SM, Laribee RN, Strahl BD. Protein modifications in transcription elongation. Biochim Biophys Acta. 2009; 1789:26–36. [PubMed: 18718879]

Gelbart ME, Kuroda MI. Drosophila dosage compensation: a complex voyage to the X chromosome. Development. 2009; 136:1399–1410. [PubMed: 19363150]

Ghamari A, van de Corput MP, Thongjuea S, van Cappellen WA, van Ijcken W, van Haren J, Soler E, Eick D, Lenhard B, Grosveld FG. In vivo live imaging of RNA polymerase II transcription factories in primary cells. Genes Dev. 2013; 27:767–777. [PubMed: 23592796]

Gilfillan GD, Straub T, de Wit E, Greil F, Lamm R, van Steensel B, Becker PB. Chromosome-wide gene-specific targeting of the Drosophila dosage compensation complex. Genes Dev. 2006; 20:858–870. [PubMed: 16547172]

Glover-Cutter K, Kim S, Espinosa J, Bentley DL. RNA polymerase II pauses and associates with pre-mRNA processing factors at both ends of genes. Nat Struct Mol Biol. 2008; 15:71–78. [PubMed: 18157150]

Jaehning JA. The Paf1 complex: platform or player in RNA polymerase II transcription? Biochim Biophys Acta. 2010; 1799:379–388. [PubMed: 20060942]

Johnsen SA. The enigmatic role of H2Bub1 in cancer. FEBS Lett. 2012; 586:1592–1601. [PubMed: 22564770]

Kelland LR. Flavopiridol, the first cyclin-dependent kinase inhibitor to enter the clinic: current status. Expert Opin Investig Drugs. 2000; 9:2903–2911.

Kim J, Guermah M, McGinty RK, Lee JS, Tang Z, Milne TA, Shilatifard A, Muir TW, Roeder RG. RAD6-Mediated transcription-coupled H2B ubiquitylation directly stimulates H3K4 methylation in human cells. Cell. 2009; 137:459–471. [PubMed: 19410543]

Kim J, Guermah M, Roeder RG. The human PAF1 complex acts in chromatin transcription elongation both independently and cooperatively with SII/TFIIS. Cell. 2010; 140:491–503. [PubMed: 20178742]

Kim J, Roeder RG. Direct Bre1-Paf1 complex interactions and RING finger-independent Bre1-Rad6 interactions mediate histone H2B ubiquitylation in yeast. J Biol Chem. 2009; 284:20582–20592. [PubMed: 19531475]

Kind J, Vaquerizas JM, Gebhardt P, Gentzel M, Luscombe NM, Bertone P, Akhtar A. Genome-wide analysis reveals MOF as a key regulator of dosage compensation and gene expression in Drosophila. Cell. 2008; 133:813–828. [PubMed: 18510926]

Langmead B, Trapnell C, Pop M, Salzberg SL. Ultrafast and memory-efficient alignment of short DNA sequences to the human genome. Genome Biol. 2009; 10:R25. [PubMed: 19261174]

Laribee RN, Fuchs SM, Strahl BD. H2B ubiquitylation in transcriptional control: a FACT-finding mission. Genes & development. 2007; 21:737–743. [PubMed: 17403775]

Laribee RN, Krogan NJ, Xiao T, Shibata Y, Hughes TR, Greenblatt JF, Strahl BD. BUR kinase selectively regulates H3 K4 trimethylation and H2B ubiquitylation through recruitment of the PAF elongation complex. Curr Biol. 2005; 15:1487–1493. [PubMed: 16040246]

Larschan E, Bishop EP, Kharchenko PV, Core LJ, Lis JT, Park PJ, Kuroda MI. X chromosome dosage compensation via enhanced transcriptional elongation in Drosophila. Nature. 2011; 471:115–118. [PubMed: 21368835]

Lee TI, Young RA. Transcriptional regulation and its misregulation in disease. Cell. 2013; 152:1237–1251. [PubMed: 23498934]

Li B, Carey M, Workman JL. The role of chromatin during transcription. Cell. 2007; 128:707–719. [PubMed: 17320508]

Li X, Li L, Pandey R, Byun JS, Gardner K, Qin Z, Dou Y. The histone acetyltransferase MOF is a key regulator of the embryonic stem cell core transcriptional network. Cell Stem Cell. 2012; 11:163–178. [PubMed: 22862943]

Lis JT. Imaging Drosophila gene activation and polymerase pausing in vivo. Nature. 2007; 450:198–202. [PubMed: 17994086]

Liu Y, Warfield L, Zhang C, Luo J, Allen J, Lang WH, Ranish J, Shokat KM, Hahn S. Phosphorylation of the transcription elongation factor Spt5 by yeast Bur1 kinase stimulates recruitment of the PAF complex. Mol Cell Biol. 2009; 29:4852–4863. [PubMed: 19581288]

Lucchesi JC, Kelly WG, Panning B. Chromatin remodeling in dosage compensation. Annu Rev Genet. 2005; 39:615–651. [PubMed: 16285873]

McGinty RK, Kim J, Chatterjee C, Roeder RG, Muir TW. Chemically ubiquitylated histone H2B stimulates hDot1L-mediated intranucleosomal methylation. Nature. 2008; 453:812–816. [PubMed: 18449190]

Minsky N, Shema E, Field Y, Schuster M, Segal E, Oren M. Monoubiquitinated H2B is associated with the transcribed region of highly expressed genes in human cells. Nat Cell Biol. 2008; 10:483–488. [PubMed: 18344985]

Nordick K, Hoffman MG, Betz JL, Jaehning JA. Direct interactions between the Paf1 complex and a cleavage and polyadenylation factor are revealed by dissociation of Paf1 from RNA polymerase II. Eukaryot Cell. 2008; 7:1158–1167. [PubMed: 18469135]

Osley MA. H2B ubiquitylation: the end is in sight. Biochim Biophys Acta. 2004; 1677:74–78. [PubMed: 15020048]

Phatnani HP, Greenleaf AL. Phosphorylation and functions of the RNA polymerase II CTD. Genes Dev. 2006; 20:2922–2936. [PubMed: 17079683]

Pirngruber J, Shchebet A, Johnsen SA. Insights into the function of the human P-TEFb component CDK9 in the regulation of chromatin modifications and co-transcriptional mRNA processing. Cell Cycle. 2009; 8:3636–3642. [PubMed: 19844166]

Piro AS, Mayekar MK, Warner MH, Davis CP, Arndt KM. Small region of Rtf1 protein can substitute for complete Paf1 complex in facilitating global histone H2B ubiquitylation in yeast. Proc Natl Acad Sci U S A. 2012; 109:10837–10842. [PubMed: 22699496]

Qin ZS, Yu J, Shen J, Maher CA, Hu M, Kalyana-Sundaram S, Chinnaiyan AM. HPeak: an HMM-based algorithm for defining read-enriched regions in ChIP-Seq data. BMC Bioinformatics. 2010; 11:369. [PubMed: 20598134]

Rahl PB, Lin CY, Seila AC, Flynn RA, McCuine S, Burge CB, Sharp PA, Young RA. c-Myc regulates transcriptional pause release. Cell. 2010; 141:432–445. [PubMed: 20434984]

Reppas NB, Wade JT, Church GM, Struhl K. The transition between transcriptional initiation and elongation in E. coli is highly variable and often rate limiting. Mol Cell. 2006; 24:747–757. [PubMed: 17157257]

Ruthenburg AJ, Li H, Patel DJ, Allis CD. Multivalent engagement of chromatin modifications by linked binding modules. Nat Rev Mol Cell Biol. 2007; 8:983–994. [PubMed: 18037899]

Sanso M, Lee KM, Viladevall L, Jacques PE, Page V, Nagy S, Racine A, St Amour CV, Zhang C, Shokat KM, et al. A positive feedback loop links opposing functions of P-TEFb/Cdk9 and histone H2B ubiquitylation to regulate transcript elongation in fission yeast. PLoS Genet. 2012; 8:e1002822. [PubMed: 22876190]

Soruco MM, Chery J, Bishop EP, Siggers T, Tolstorukov MY, Leydon AR, Sugden AU, Goebel K, Feng J, Xia P, et al. The CLAMP protein links the MSL complex to the X chromosome during Drosophila dosage compensation. Genes Dev. 2013; 27:1551–1556. [PubMed: 23873939]

Straub T, Becker PB. Comment on “Drosophila dosage compensation involves enhanced Pol II recruitment to male X-linked promoters”. Science. 2013; 340:273. [PubMed: 23599464]

Suganuma T, Workman JL. Chromatin and signaling. Curr Opin Cell Biol. 2013; 25:322–326. [PubMed: 23498660]

Sural TH, Peng S, Li B, Workman JL, Park PJ, Kuroda MI. The MSL3 chromodomain directs a key targeting step for dosage compensation of the Drosophila melanogaster X chromosome. Nat Struct Mol Biol. 2008; 15:1318–1325. [PubMed: 19029895]

Tomson BN, Arndt KM. The many roles of the conserved eukaryotic Paf1 complex in regulating transcription, histone modifications, and disease states. Biochim Biophys Acta. 2013; 1829:116–126. [PubMed: 22982193]

Tomson BN, Davis CP, Warner MH, Arndt KM. Identification of a role for histone H2B ubiquitylation in noncoding RNA 3'-end formation through mutational analysis of Rtf1 in Saccharomyces cerevisiae. Genetics. 2011; 188:273–289. [PubMed: 21441211]

Trujillo KM, Osley MA. A role for H2B ubiquitylation in DNA replication. Mol Cell. 2012; 48:734–746. [PubMed: 23103252]

Tweedie-Cullen RY, Reck JM, Mansuy IM. Comprehensive mapping of post-translational modifications on synaptic, nuclear, and histone proteins in the adult mouse brain. J Proteome Res. 2009; 8:4966–4982. [PubMed: 19737024]

Vaquerizas JM, Cavalli FM, Conrad T, Akhtar A, Luscombe NM. Response to Comments on "Drosophila Dosage Compensation Involves Enhanced Pol II Recruitment to Male X-Linked Promoters". Science. 2013; 340:273. [PubMed: 23599465]

Weake VM, Workman JL. Histone ubiquitination: triggering gene activity. Molecular cell. 2008; 29:653–663. [PubMed: 18374642]

Wood A, Schneider J, Dover J, Johnston M, Shilatifard A. The Bur1/Bur2 complex is required for histone H2B monoubiquitination by Rad6/Bre1 and histone methylation by COMPASS. Mol Cell. 2005; 20:589–599. [PubMed: 16307922]

Wu L, Zee BM, Wang Y, Garcia BA, Dou Y. The RING finger protein MSL2 in the MOF complex is an E3 ubiquitin ligase for H2B K34 and is involved in crosstalk with H3 K4 and K79 methylation. Mol Cell. 2011; 43:132–144. [PubMed: 21726816]

Zeitlinger J, Stark A, Kellis M, Hong JW, Nechaev S, Adelman K, Levine M, Young RA. RNA polymerase stalling at developmental control genes in the Drosophila melanogaster embryo. Nat Genet. 2007; 39:1512–1516. [PubMed: 17994019]

Zhang F, Yu X. WAC, a functional partner of RNF20/40, regulates histone H2B ubiquitination and gene transcription. Mol Cell. 2011; 41:384–397. [PubMed: 21329877]

Zhou K, Kuo WH, Fillingham J, Greenblatt JF. Control of transcriptional elongation and cotranscriptional histone modification by the yeast BUR kinase substrate Spt5. Proc Natl Acad Sci U S A. 2009; 106:6956–6961. [PubMed: 19365074]

Zhu B, Zheng Y, Pham AD, Mandal SS, Erdjument-Bromage H, Tempst P, Reinberg D. Monoubiquitination of human histone H2B: the factors involved and their roles in HOX gene regulation. Mol Cell. 2005; 20:601–611. [PubMed: 16307923]

HIGHLIGHTS

- H2BK34ub by the MSL complex is prevalent in mammalian cells.
- The MSL complex regulates co-transcriptional histone modifications.
- The MSL, RNF20/40 and PAF1 complexes cooperate to regulate pTEFb.
- The MSL complex regulates transcription by promoting RNA Pol II processivity.

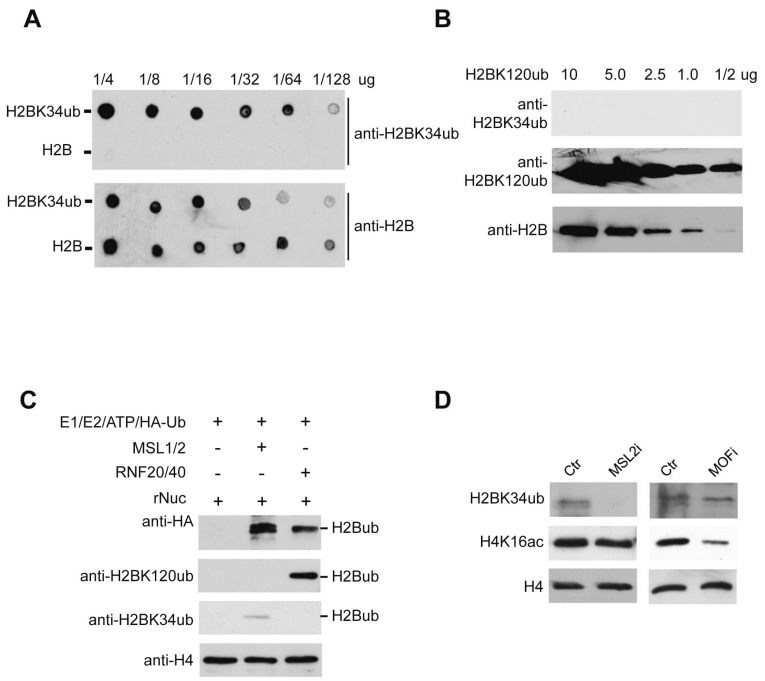

Figure 1. Confirmation of MSL2 mediated H2BK34ub *in vitro* and *in vivo* using a newly development anti-H2BK34ub antibody

A. Dot-blot for unmodified H2B or branched H2BK34ub peptides using antibodies as indicated on right. Quantities of H2B or H2BK34ub peptides were indicated on top. **B.** Immunoblot for the chemically synthesized H2BK120ub protein using antibodies indicated on left. **C.** *In vitro* ubiquitylation assay using either MSL1/2 or RNF20/40 as the E3 ubiquitin ligase as indicated on top. Recombinant nucleosomes were used as the substrates. Ubiquitylated H2B was detected by anti-HA, anti-H2BK120ub or anti-H2BK34ub antibodies as indicated on left. Immunoblot using anti-H4 antibody was used as the loading control. **D.** Immunoblot for total H2BK34ub, H4K16ac and H4 from HeLa cells treated with or without MSL2 or MOF siRNAs as indicated on top. See also Figure S1.

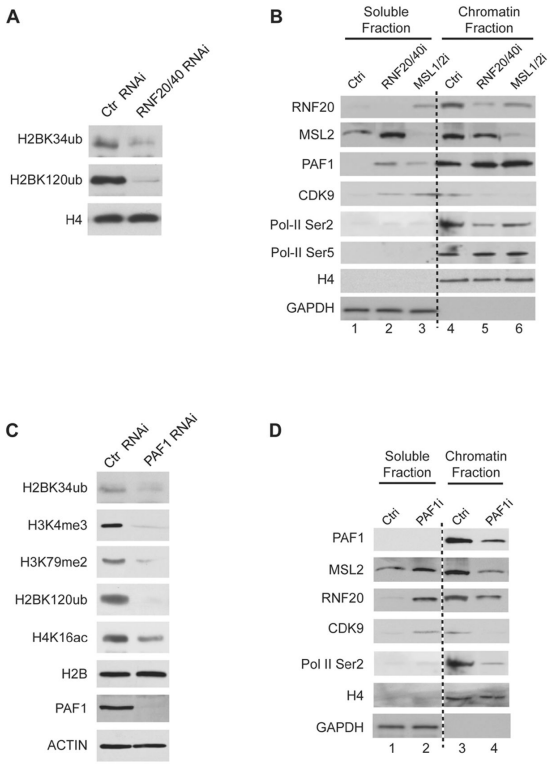

Figure 2. Mutual dependence of chromatin binding by MSL, RNF20/40 and PAF1C

A. Immunoblot for histones isolated from HeLa cells after control or RNF20 and RNF40 siRNA treatments. **B.** Immunoblot for histones isolated from HeLa cells after RNF20/40 or MSL1/2 knockdown. **C.** Immunoblot for histones isolated from HeLa cells after control or PAF1C siRNA treatment. **D.** Immunoblot for proteins in soluble and chromatin fractions after control and PAF1 knockdown. For A–D, antibodies were shown on left. Immunoblot for H4 GAPDH were used as controls to indicate good separation of soluble and chromatin fractions in B and D. See also Figure S2.

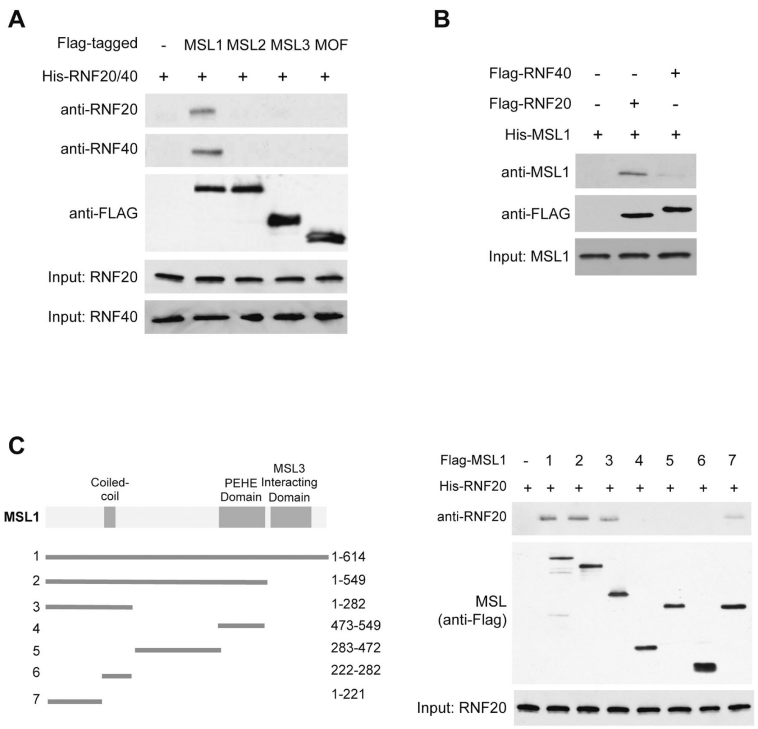

Figure 3. MSL1 directly interacts with RNF20

A. Flag-tagged MSL1, MSL2, MSL3 or MOF was individually incubated with the His-tagged RNF20/40 complex and subject to M2-agarose purification. The immune-precipitated (IP) proteins were blotted with antibodies indicated on left. Input controls for RNF20 and RNF40 were at bottom. **B.** Flag-tagged RNF40 or RNF20 was individually incubated with His-MSL1 and subject to M2-agarose purification. Immunoblot for the IPed proteins were performed using antibodies on left. **C.** Left, schematics for MSL1 truncation mutants used in the pull down assays. Right, immunoblots using antibodies indicated on right.

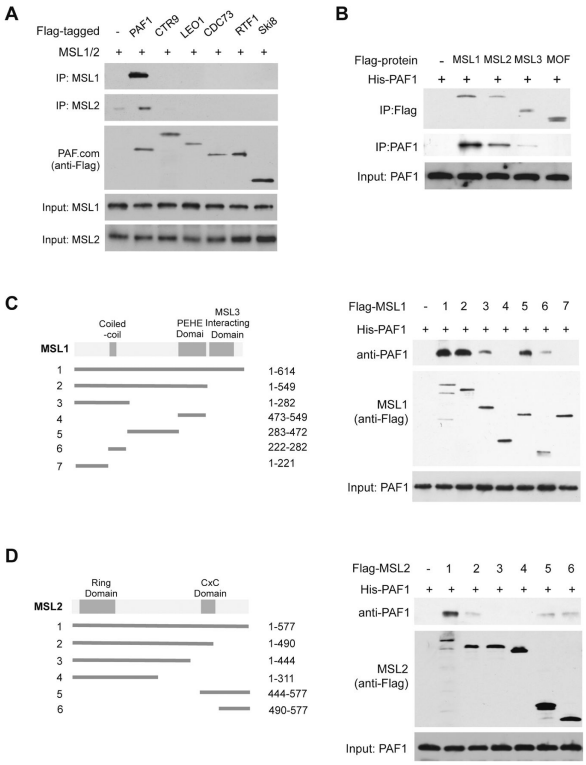

Figure 4. The MSL1/2 complex directly interacts with PAF1

A. Flag-tagged PAF1, CTR9, LEO1, CDC73, RTF1 or Ski8 was individually incubated with the recombinant MSL1/2 complex and subject to M2 purification. Immunoblots for IP and inputs were shown using antibodies indicated on left. **B.** Flag-tagged MSL1, MSL2, MSL3 or MOF was incubated with the PAF1 protein and subject to M2 purification. Immunoblot using antibodies indicated on left was shown. **C,D.** Left, schematics for MSL1 (C) and MSL2 (D) truncation mutants used in the IP experiments. Right, immunoblot for IPed proteins using truncated proteins and recombinant PAF1 proteins as indicated on top.

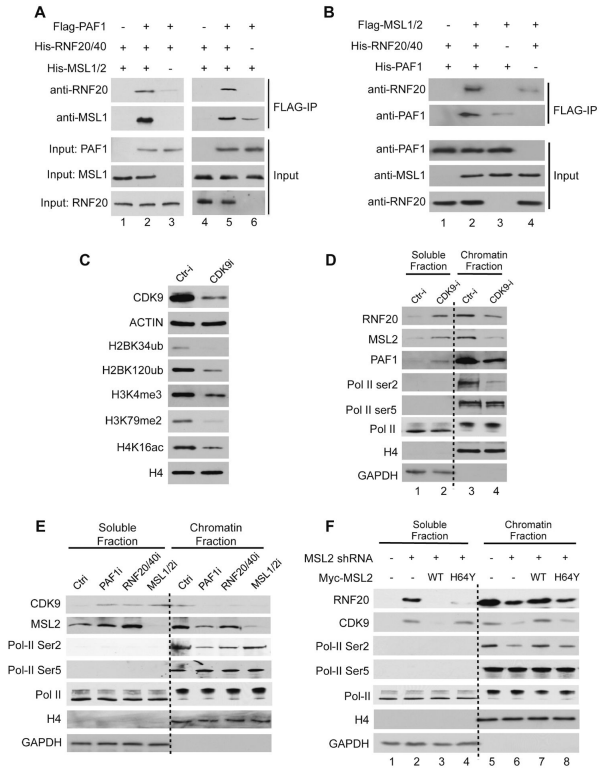

Figure 5. Binary interactions of PAF1C, RNF20/40 and MSL complexes stabilize their interactions and regulate pTEFb chromatin recruitment

A. Flag-tagged PAF1 was incubated with His-tagged RNF20/40 or MSL1/2 as indicated on top. Immunoblot was performed for IP and input proteins using antibodies indicated on left. **B.** Flag-tagged MSL1/MSL2 heterodimer (Flag-MSL1) was incubated with His-tagged RNF20/40 or PAF1 as indicated on top. Immunoblot was performed for IP and input proteins. **C.** Immunoblot for histones isolated from HeLa cells treated with control or CDK9 siRNAs. Antibodies were indicated on left. **D.** Immunoblot for proteins distributed in soluble vs. chromatin fractions in cells treated with control or CDK9 siRNAs. **E.** Immunoblot for proteins distributed in soluble vs. chromatin fractions in cells treated with control, PAF1, RNF20/40, MSL1/2 siRNAs as indicated on top. **F.** Immunoblot for proteins distribution after MSL2 knockdown followed by overexpression of Myc-tagged RNAi resistant MSL2 or MSL2 ^{H64Y} mutant as indicated on top. For **A–F**, antibodies were indicated on left. See also Figure S3.

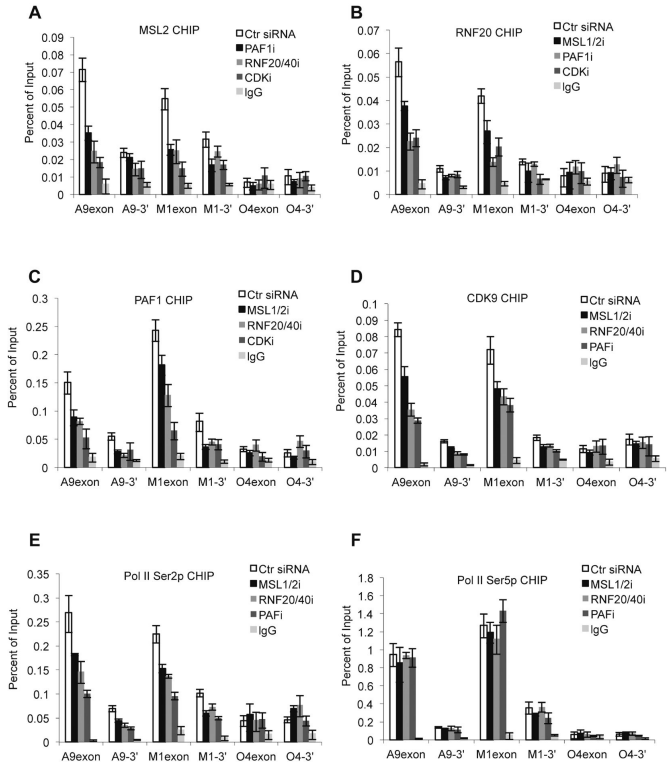

Figure 6. Interplays of the MSL complex with transcription elongation factors at *Hoxa9* and *Meis1* loci in cells

HeLa cells were treated with control, PAF1, RNF20/40 or CDK9 siRNAs and subject to CHIP analyses for MSL2 (**A**), RNF20 (**B**), PAF1 (**C**), CDK9 (**D**), Pol II Ser2p (**E**) and Pol II Ser5p **(F)**. Primer sets for *HOXA9 (A9)*, *MEIS1 (M1)* and *Oct4 (O4)* used in ChIP assays were indicated on bottom. Signals for each experiment were normalized to 5% input. Means and standard deviations (as error bars) from at least three independent experiments were presented.

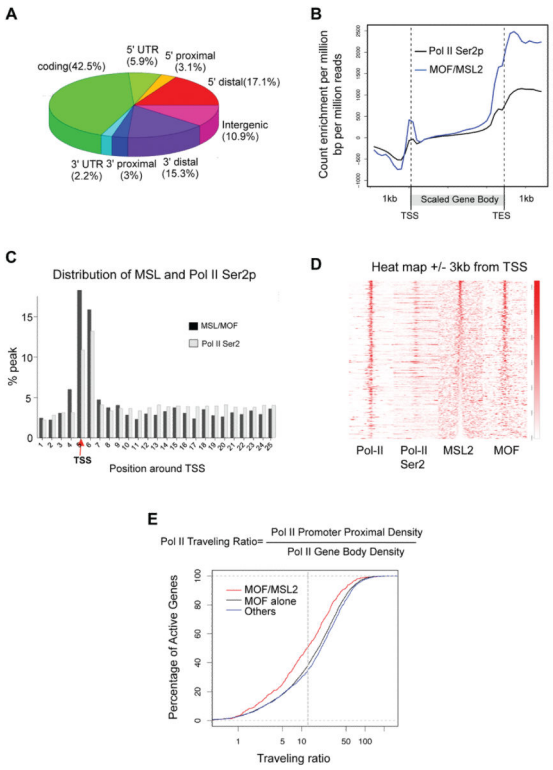

Figure 7. Genome-wide analyses of Msl2 target genes

A. Genome-wide distribution of Msl2 relative to gene structure. Relative ratio of Msl2 peaks at each defined genomic region versus total peaks was indicated as %. **B.** Genome average of Mof/Msl2 (blue) and Pol II Ser2p (black) binding on scaled genes. Y-axis, count enrichment after normalization against gene length and read counts. **C.** Bar plot showing distribution of the Msl complex, as defined by the joint peaks for Mof and Msl2, and Pol II Ser2phos relative to nearest TSS. Each bin (X-axis) represents a 500bp region. **D.** Heat map representation of ChIP-seq peaks for Pol II, Pol II Ser2, Msl2 and Mof at genes bound by the Msl complex within ±3.5kb of TSS. The rank was ordered from highest Msl2 to lowest Msl2 binding. Red means enrichment, white means no enrichment. Total enrichment within ±3.5kb of TSS was calculated. **E.** Distribution of traveling ratio for all genes with TR values. Traveling ratio for genes was calculated as described previously (Rahl et al., 2010). Cumulative distribution function (CDF) of traveling ratio for genes bound by the Mof/Msl2 complex (red), Mof alone (black) and non-Mof targets (blue) were plotted. *p*-values (Wilcoxon Signed-rank test) for TR difference were 4.023e-13 (red-black), 4.391e-13 (red-blue). See also Figure S4–6.